JOURNAL OF MATERIALS SCIENCE 21 (1986) 2803–2811

# Effect of heat treatment on precipitation behaviour and high temperature strength in a wrought Co-base superalloy

HIROSHI IIZUKA, MANABU TANAKA
*Department of Mechanical Engineering for Production, Mining College, Akita University, Tegatagakuen-cho 1-1, Akita 010, Japan*

The effects of solution and ageing temperatures on the grain boundary reaction as well as on matrix precipitation in the interior of the grains were investigated using wrought Co-base superalloy HS-21. The grain boundary reaction occurred during furnace-cooling after solution-heating. The phase that precipitated in the grain boundary reactions nodule was $M_{23}C_6$ carbide. It also occurred during ageing after solution treatment, but the extent of it was considerably influenced by cooling procedure after solution heating. The activation energy of the grain boundary reaction was 244 kJ mol$^{-1}$ for the early stage of the grain boundary reaction in HS-21 alloy, and was considered to be the activation energy of grain boundary diffusion of chromium. The extent of the matrix precipitation that occurred during ageing was also influenced by the cooling procedure. Creep rupture tests were carried out at 1088 K in air. An excellent combination of long rupture life and large ductility was attained on a specimen, which involved both the grain boundary reaction nodules (about 7% in area fraction) and the matrix precipitates. The improvement of creep rupture properties results from the retardation of brittle intergranular fracture, which is achieved by grain boundary serration owing to the grain boundary reaction and by the increase of strength in the interior of grain due to the matrix precipitation.

## 1. Introduction

Co-base heat resisting superalloy HS-21 has excellent corrosion and thermal fatigue resistance, and it is used for high temperature applications [1], such as industrial turbine nozzles and metallic moulds for hot presses, and recently for biomedical implant applications [2]. The effects of solution treatment [3] and ageing treatment [4–6] on creep rupture strength have been investigated for cast HS-21. Moreover, precipitation behaviour [7] and allotropic transformation from fcc to hcp phase during ageing has been studied for wrought alloy [8, 9]. Since HS-21 alloy contains relatively large amounts of carbon (about 0.25 wt%), grain boundary reaction (GBR) occurs readily during a heat treatment in this alloy as well as in austenitic heat resisting steels with large amount of carbon and nitrogen [10–12]. The phase that precipitated in the GBR was $M_{23}C_6$ carbide [6, 7]. It has been known in austenitic heat resisting steels that grain boundary serration occurs considerably in the early stage of the GBR [13]. A few studies revealed that creep rupture strength is significantly affected by the occurrence of GBR in HS-21 alloy [4, 7]. However, neither the initiation mechanism of the GBR nor its effect in mechanical properties has sufficiently been studied in HS-21 alloy.

In this study, the effect of heat treatment on the GBR as well as on the matrix precipitation in the interior of grain was investigated for wrought Co-base superalloy HS-21. Then, a discussion was made on the correlation between the occurrence of the GBR and the matrix precipitation. Further, the strengthening mechanism by the GBR and the matrix precipitation was examined by creep rupture tests performed at 1088 K in air.

## 2. Material and experimental procedures

Co-base heat resisting superalloy HS-21, which was vacuum cast in 30 kg ingots, was wrought into rods of 16 mm diameter at 1423 K. The chemical composition of HS-21 alloy is listed in Table I. GBR occurs markedly during furnace cooling after solution heating. Samples were furnace cooled to a certain temperature after solution heating and then quenched into ice–water mixture maintained at 273 K. The effect of solution temperature on the GBR was also examine on samples furnace cooled after heating for 3.6 ksec at the solution temperature in the range from 1448 to 1573 K. GBR also occurs markedly during ageing treatment. Other samples were cooled by three kinds of cooling procedures after solution treatment for

TABLE I Chemical composition of HS-21 alloy used (wt %)

| Material | C | Cr | Ni | Mo | Si | Mn | Fe | B | P | S | Co |
|---|---|---|---|---|---|---|---|---|---|---|---|
| HS-21 | 0.27 | 26.71 | 2.37 | 5.42 | 0.59 | 0.64 | 0.09 | 0.003 | < 0.005 | 0.007 | balance |

0022–2461/86 $03.00 + .12 

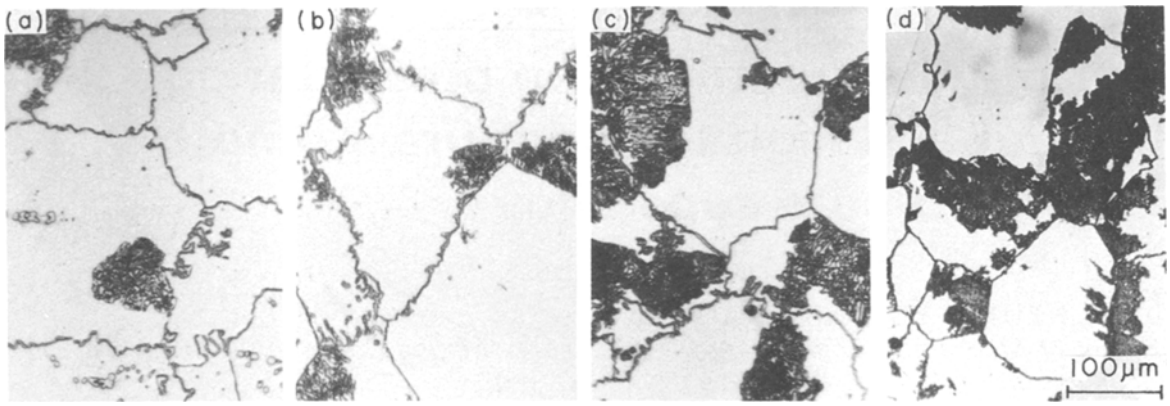


*Figure 1* Optical micrographs of HS-21 alloy furnace cooled to (a) 1323 K, (b) 1223 K, (c) 973 K and (d) room temperature, after solution treatment for 3.64 ksec at 1523 K.

3.6 ksec at 1523 K, namely, directly "quenched" to the ageing temperature, water quenched, or air cooled to room temperature.

The cooling rate in the furnace was measured using a thermocouple, and it was about 3 K $min^{-1}$ for the temperature range from 1300 to 1000 K. The cooling rate in the direct quenching was not likely to be high as in typical quenching treatments. Ageing treatment was then performed in the temperature range from 873 to 1323 K. The amount of GBR (in area fraction) was measured by linear analysis. The extent of matrix precipitation was estimated by the increase of micro-Vickers hardness (load 5N) in the interior of grain. Microstructures of the samples were also observed by means of transmission electron microscopy (TEM). The thin foils for TEM were prepared by electro-polishing using a solution of ethanol–15% perchloric acid. Moreover, some samples were examined by X-ray diffraction to obtain the volume fraction of α-Co phase (h c p) in β-Co solid solution (f c c) [14]. Creep rupture tests were carried out at 1088 K in air. Specimens were machined from the three kinds of heat treated samples, which had different extents of GBR. The gauge length and the diameter of the specimens were 30 and 6 mm, respectively.

## 3. Results and discussion

### 3.1. Grain boundary reaction (GBR) during furnace cooling

It was found that residual carbides in HS-21 alloy used in this study were entirely taken into solid solution during heating for 3.6 ksec at 1523 K. GBR occurred considerably during furnace cooling from the solution temperature. Fig. 1a shows the microstructure of a sample which was furnace cooled to 1323 K and then water quenched. GBR nodules developed to about 7% in area fraction. Fig. 1b shows the microstructure of a sample which was furnace cooled to 1223 K and the amount of GBR was about 19%. The amount of GBR in a sample which was furnace cooled to 973 K, was about 28% (Fig. 1c). It was almost equal to that of a sample which was furnace cooled to room temperature, as shown in Fig. 1d. It should also be noted that the grain boundary was considerably serrated in samples with an amount of above about 7% GBR (in area fraction).

Fig. 2 shows the change in the amount of GBR during furnace cooling after solution treatment for 3.6 ksec at 1523 K. The GBR occurred below about 1373 K during furnace cooling. The amount of it increased with the decrease of temperature in the range from 1373 to 1173 K, and then, it increased no more below about 1173 K.

The microstructure of a sample which was furnace cooled to room temperature after solution heating for 3.6 ksec at 1523 K, was also observed by TEM. Dislocation density was very low (about 1.3 × $10^{11}$ $m^{-2}$) and very few stacking faults were observed in this sample. Matrix precipitates could not be observed in the grain, while GBR nodules and coarse precipitates occurred at the grain boundary. The data obtained by X-ray analysis showed that these precipitates were all

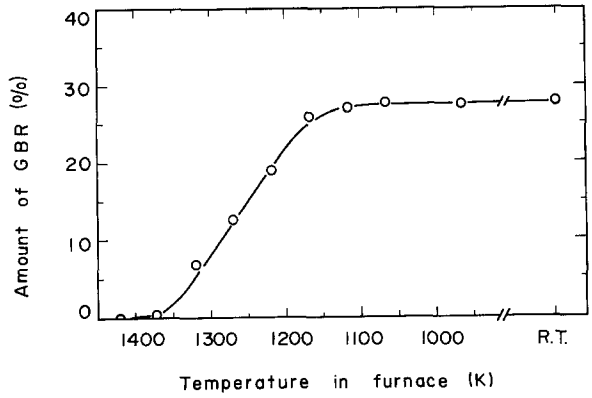


*Figure 2* Amount of grain boundary reaction (GBR) occurring in HS-21 alloy during furnace cooling after solution treatment for 3.6 ksec at 1523 K. Cooling rate 3 K $min^{-1}$ (1300 to 1000 K).

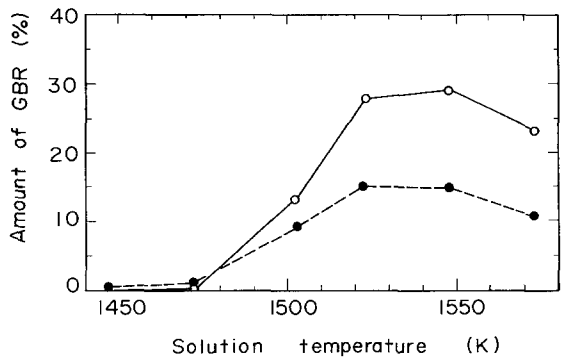


*Figure 3* Amount of grain boundary reaction (GBR) in two kinds of HS-21 alloys solution heated for 3.6 ksec at various temperatures and then furnace cooled. (○) HS-21 (0.27% C), (●) low carbon HS-21 (0.20% C).

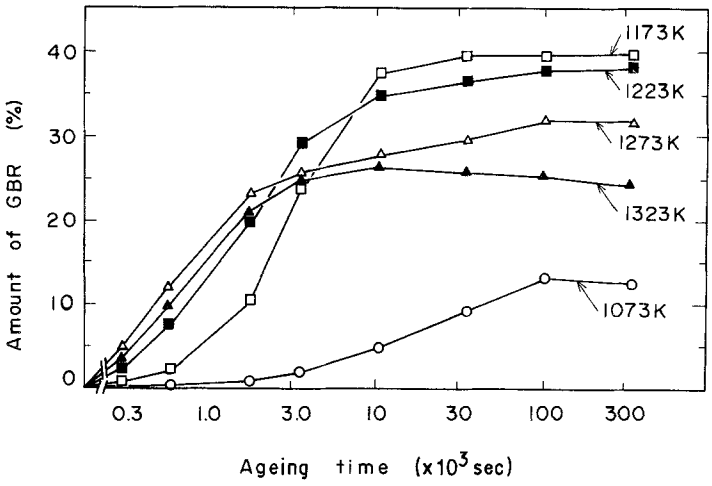


*Figure 4* Amount of grain boundary reaction (GBR) in HS-21 alloy occurring during ageing in directly quenched samples after solution treatment for 3.6 ksec at 1523 K.

$M_{23}C_6$ carbides. The matrix phase of the furnace cooling sample consisted of $\beta$-Co (fcc) solid solution (about 70%) and $\alpha$-Co (hcp) solid solution (about 30%). Further, the matrix phase of the as water-quenched and the as air-cooled samples was identified to be $\beta$-Co solid solution alone.

The extent of GBR was also affected by the solution temperature. Fig. 3 shows the relationship between the solution temperature and the amount of GBR that occurred during furnace cooling to room temperature. The GBR occurred considerably in the solution temperature range from 1523 to 1558 K. Below about 1523 K, residual carbides still remained in the grain, and the amount of GBR was relatively small, while eutectic constituent developed at the triple junctions of grain boundaries above about 1573 K, so that the amount of GBR decreased. Fig. 3 also shows the experimental data on another charge of HS-21 alloy with a smaller carbon content (0.20%). The amount of GBR in this alloy was about half that in the alloy with 0.27% C.

## 3.2. Grain boundary reaction (GBR) during ageing

Samples were directly "quenched" from 1523 K into a furnace maintained in the temperature range from 873 to 1323 K and aged after solution treatment for 3.6 ksec at 1523 K. Fig. 4 shows the amount of GBR occurring during ageing in the directly quenched samples. The GBR occurred considerably in the temperature range from 1173 to 1323 K. The maximum amount of it, about 39%, was attained by ageing at 1173 K, while the GBR proceeded most rapidly at 1273 K.

Fig. 5 shows the transmission electron micrograph of a sample aged for 1.8 ksec at 1273 K after solution treatment. From selected area diffraction patterns, all precipitates were identified to be $M_{23}C_6$ carbide. The GBR nodule contained rod-like $M_{23}C_6$ carbides, and coarse $M_{23}C_6$ carbides existed at the grain boundary. The matrix of the GBR nodules substantially consisted of $\beta$-Co solid solution. Moreover, the orientation of $M_{23}C_6$ carbides in the nodule was in parallel with that of the matrix in the nodule, $(\bar{1}\,1\,1)_{M_{23}C_6} \| (\bar{1}\,1\,1)_{\beta\text{-Co}}$, $[0\,\bar{1}\,1]_{M_{23}C_6} \| [0\,\bar{1}\,1]_{\beta\text{-Co}}$. The analysis of electron diffraction pattern showed tht the orientation of the matrix in the nodule was identical with that of the neighbouring grain, $(2\,1\,1)_{\beta\text{-Co}}$, while the orientation of the grain in front of the GBR nodule was $(1\,1\,1)_{\beta\text{-Co}}$ and was different from that of the nodule. It was confirmed

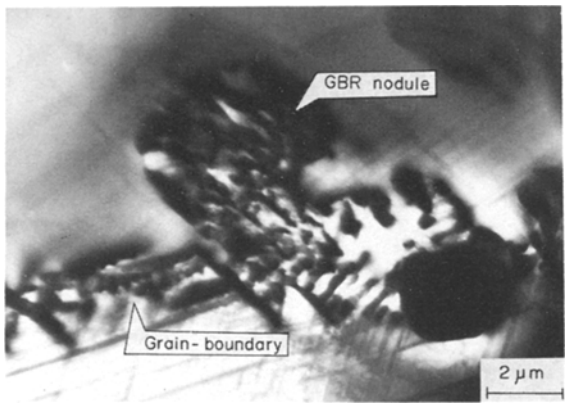


*Figure 5* Transmission electron micrograph of grain boundary reaction (GBR) region in HS-21 alloy which was directly quenched after solution treatment for 3.6 ksec at 1523 K and aged for 1.8 ksec at 1273 K.

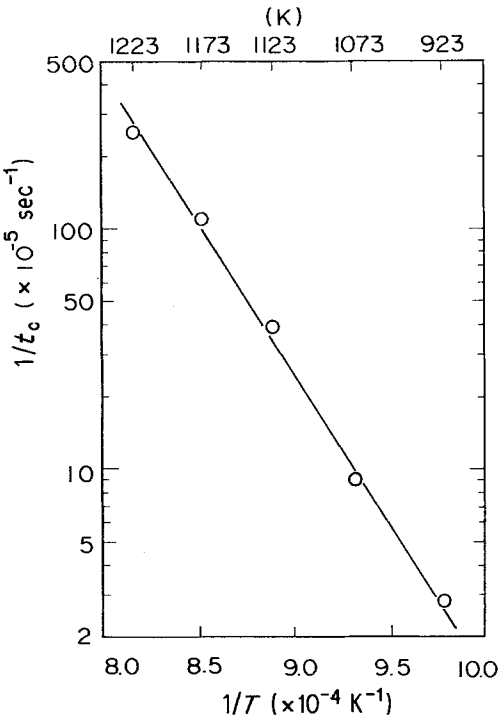


*Figure 6* Activation energy for grain boundary reaction (GBR). $t_c$ = time to 5% GBR, $Q$ = 244 kJ mol$^{-1}$.

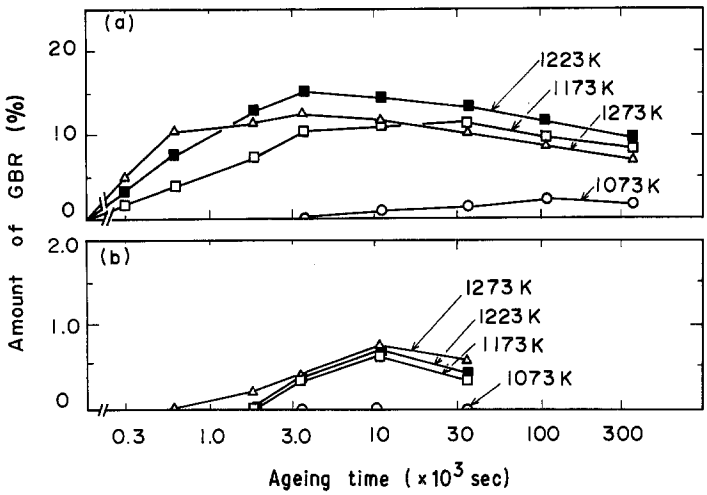


*Figure 7* Effect of cooling procedure on amount of grain boundary reaction (GBR) in HS-21 alloy occurring during ageing after solution treatment for 3.6 ksec at 1523 K. (a) air cooled, (b) water quenched.

that the GBR nodule is not formed as a result of eutectoid reaction.

Activation energy ($Q$) in the early stage of GBR can be calculated using the experimental result shown in Fig. 4. Fig. 6 shows the semilog relationship between a reciprocal of ageing time and a reciprocal of time to 5% GBR. The value of $Q$ calculated was 244 kJ mol$^{-1}$. The value of $Q$ obtained is lower than that of self-diffusion of chromium (307 $\pm$ 17 kJ mol$^{-1}$) [15]. The activation energy of grain boundary diffusion is known to be three-quarters or one-half of that of self-diffusion. Therefore, the value obtained above is considered to be the activation energy of grain boundary diffusion for chromium.

### 3.3. Effect of cooling procedure on GBR and matrix precipitation

The effect of cooling procedure on GBR and matrix precipitation during ageing was also investigated. Fig. 7 shows the effect of cooling procedure on the occurrence of GBR. The experimental results obtained on directly quenched samples were already shown in Fig. 4. It is evident from these figures that the GBR was considerably influenced by the cooling procedure after solution heating. The maximum amount of GBR occurred in the directly quenched samples. In the air cooled samples, the extent of GBR increased no more in the relatively early stage of ageing compared with the directly quenched one, and maximum amount of it was obtained by ageing at 1223 K. The apparent amount of GBR slightly decreased for a long time ageing due to the spheroidization of rod-like $M_{23}C_6$ carbides., Fig. 7b shows the extent of GBR in the water quenched sample. A very small amount of GBR occurred even at the higher temperature above about 1173 K, and GBR was not observed on samples aged at temperatures below about 1073 K. Fig. 8 shows the maximum amount of GBR occurring during ageing at various temperatures. The amount of GBR in the air cooled sample was about one-third of that of the directly quenched one. The amount of it in the water quenched one was less than 1.0%. These results revealed that the effect of the cooling procedure is extremely large on the occurrence of GBR during ageing.

Fig. 9 shows the optical microstructures of samples aged for 36 ksec at 1073, 1173 and 1273 K. In the directly quenched samples, the matrix precipitation occurred and the GBR hardly observed at the lower ageing temperature (1073 K) (Fig. 9a). However, a larger amount of GBR and a smaller extent of matrix precipitates were observed on the sample aged at 1173 K (Fig. 9b). Above about 1273 K, very few precipitates could be observed in the interior of grain (Fig. 9c). In the air cooled samples, matrix precipitation dominantly occurred and the GBR was not observed on the sample aged at 1073 K. Both the GBR and the matrix precipitation were observed in the sample aged at 1173 K. The matrix precipitation still occurred during ageing at 1273 K. In the water quenched samples, the GBR was hardly observed at all ageing temperatures, as shown in Fig. 9g to i, while the matrix precipitation occurred considerably even during ageing at 1273 K.

The extent of matrix precipitation can be estimated by measuring the increment of matrix hardness during ageing. Fig. 10 shows the contours of equivalent hardness with the TTT curves of 5% GBR which gives a measure of the initiation of GBR. The TTT curves were obtained from the experimental results shown in

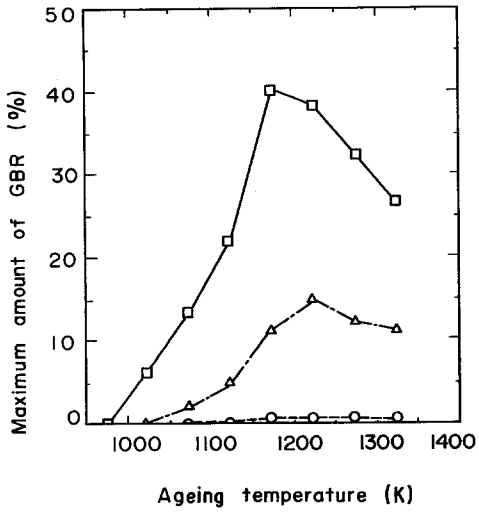


*Figure 8* Effect of cooling procedure on maximum amount of grain boundary reaction (GBR) in HS-21 alloy occurring during ageing after solution treatment for 3.6 ksec at 1523 K. (□) direct quenching, (△) air cooled, (○) water quenched.

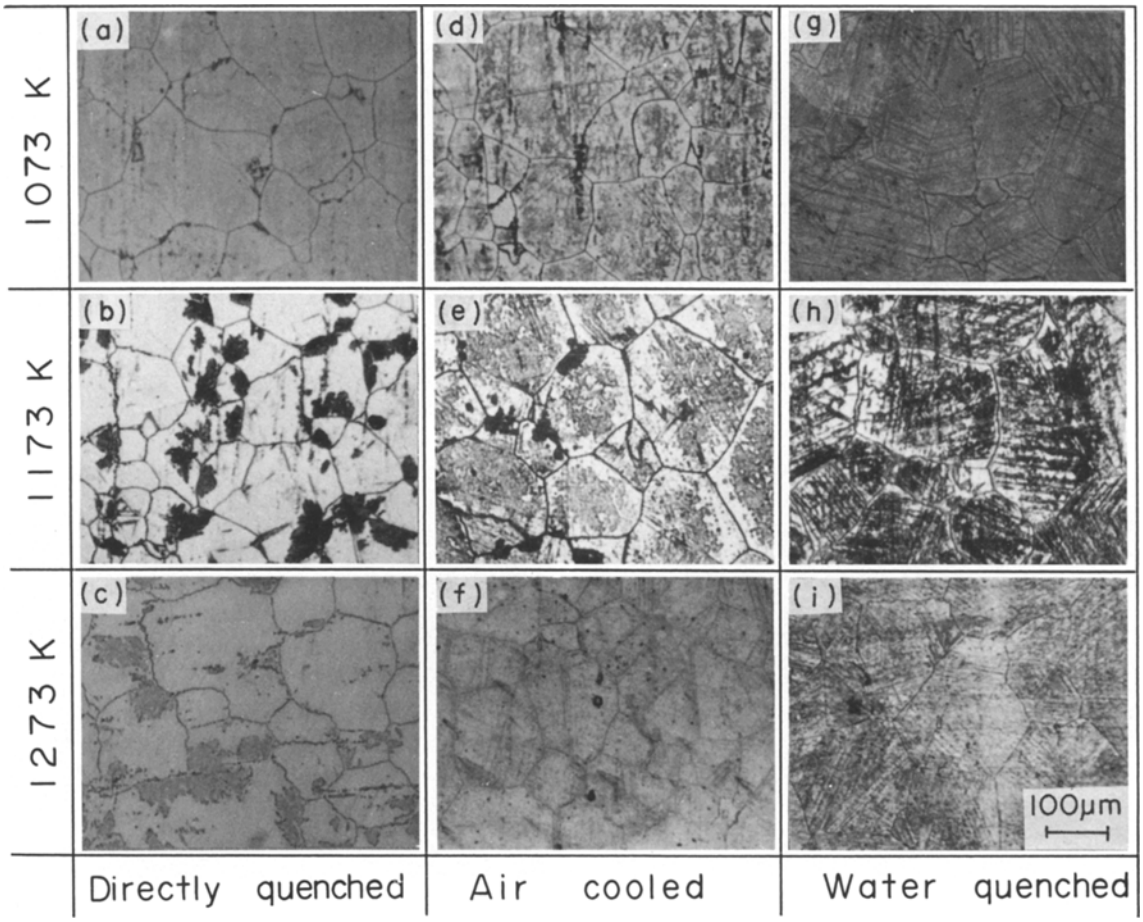


*Figure 9* Microstructures of HS-21 alloy aged for 36 ksec at 1073 to 1273 K after solution treatment for 3.6 ksec at 1523 K.

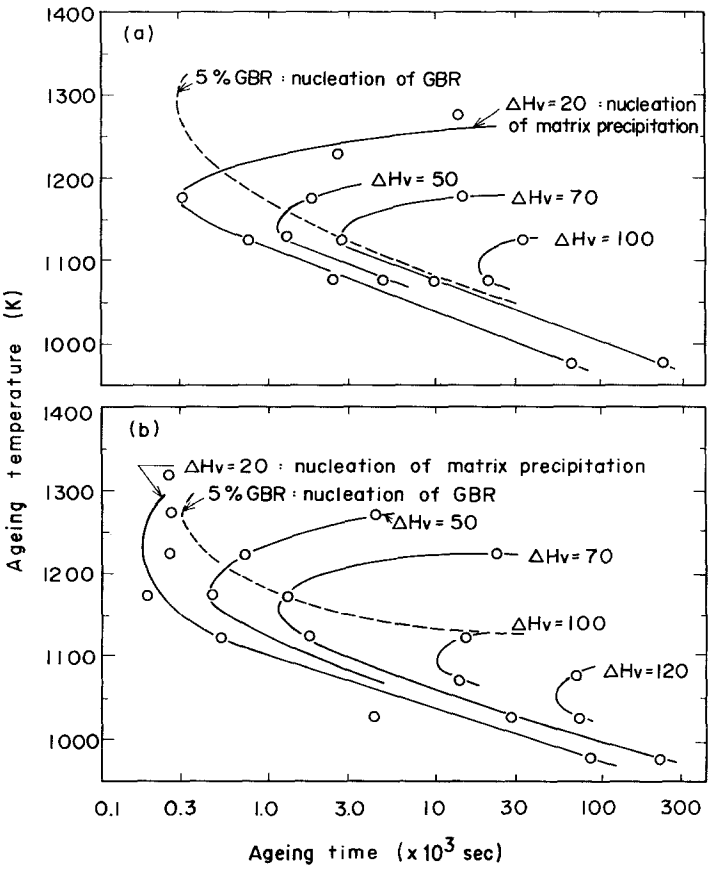


*Figure 10* Relation between grain boundary reaction (GBR) and matrix precipitation of HS-21 alloy which was solution treated for 3.6 ksec at 1523 K and aged at various temperatures. Hardness before ageing 330 Hv. (a) Direct quenching, (b) air cooled.

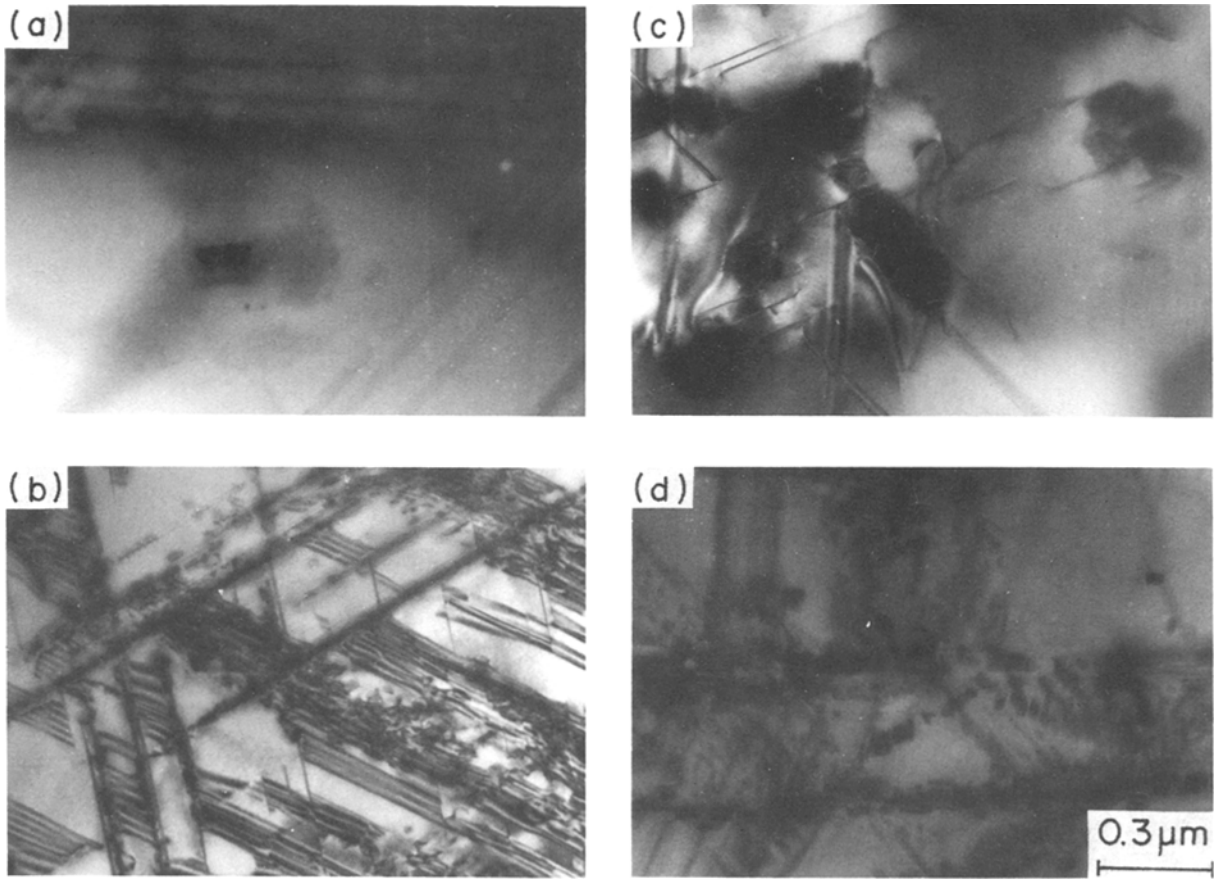


*Figure 11* Effect of ageing temperature and cooling procedure on matrix precipitation in the interior of grains of HS-21 alloy after solution treatment for 3.6 ksec at 1523 K. (a) and (b) show micrographs of directly quenched samples aged for 1.8 ksec at 1273 K and 10.8 ksec at 1073 K, respectively. (c) and (d) show micrographs of water quenched samples aged for 1.8 ksec at 1273 K and 10.8 ksec at 1073 K, respectively.

Fig. 4 and Fig. 7a. The initiation of matrix precipitation was assumed to correspond to the increase of matrix hardness ($\Delta$ Hv) by 20 Hv from the hardness before ageing, so that the comparison between the presence of the GBR and the matrix precipitation mentioned above was more clearly indicated.

Fig. 11 shows the transmission electron micrographs of aged samples. Many stacking faults were observed in the micrographs of the samples aged for 10.8 ksec at 1073 K, as shown in Fig. 11b and d. $M_{23}C_6$ carbides were dominantly precipitated on the stacking faults, and no association with dislocations was observed. The mechanism of the $M_{23}C_6$ carbide precipitation was explained by "Suzuki segregation" [6].

While, few stacking faults were observed in the micrographs of the samples aged for 1.8 ksec at 1273 K. Instead, coarse $M_{23}C_6$ carbides precipitated dominantly on dislocations, as shown in Fig. 11a and c, and no association with the stacking faults was observed. Therefore, the difference in nucleation mechanism of the $M_{23}C_6$ precipitates was explained by thermodynamic stability of the fcc phase and subsequent energy change for stacking fault formation [6].

The observation shown in Fig. 11 also indicates that the amount of $M_{23}C_6$ carbides in the water quenched samples was larger than that in the samples directly quenched. These observations and the results shown in Figs 9 and 10 imply that the amount of $M_{23}C_6$ carbides increased with the increase of cooling rate after solution heating. The $M_{23}C_6$ carbides were precipitated almost on dislocations or stacking faults, as mentioned above. Dislocation density was then measured using TEM photographs for each sample before ageing. The dislocation density was $3.8 \times 10^{12}\,m^{-2}$ for a sample water quenched after solution heating, $5.2 \times 10^{11}\,m^{-2}$ for a sample air cooled after solution heating and $1.3 \times 10^{11}\,m^{-2}$ for a sample furnace cooled after solution heating. Therefore, the difference of the extent of matrix precipitation by the cooling procedure in the early stage of ageing is explained by the difference of dislocation density in the structure. If the matrix precipitates considerably increase, the driving force for GBR is reduced due to a decrease of the supersaturation of carbon in matrix, so that the amount of GBR decreases. The same discussion is also applicable to the effect of ageing temperature on the occurrence of GBR. The GBR proceeds in the early stage of ageing at high temperatures around 1223 K, as shown in Fig. 4. In general, the diffusion of atoms is easy at high temperature, while the solubility limit of carbon increases with the rise of temperature, so that the driving force for GBR decreases with increasing temperature. In addition to this, the matrix precipitation occurs considerably on stacking faults in the samples aged at lower temperatures below about 1173 K (Fig. 11), and decreases the carbon content dissolved in the matrix. Thus, the temperature dependence of GBR, shown in

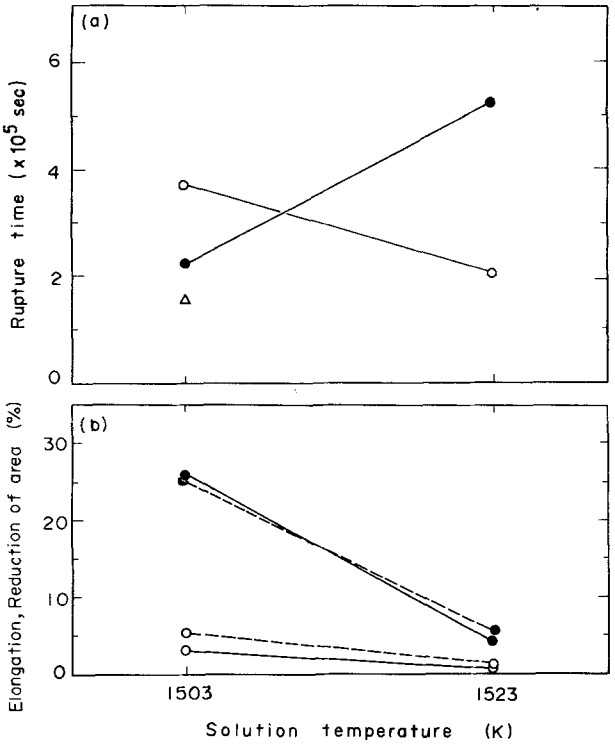


*Figure 12* Effect of solution temperature on creep rupture properties of HS-21 alloy at 1088 K, 137 MPa. (●) 1503 or 1523 K for 3.6 ksec, furnace cooled to 1323 K then water quenched, (○) 1503 or 1523 K for 3.6 ksec then water quenched, (△) 1503 K for 3.6 ksec then furnace cooled. (——) reduction of area, RA; (– – –) elongation, E.

Fig. 10, is explained by the concept of driving force mentioned above.

### 3.4. Creep rupture properties

Creep rupture tests were carried out at 1088 K in air using specimens which showed different extents of GBR. The creep rupture specimens were machined from the three kinds of samples which were subjected to the following heat treatments. Samples of the first group were furnace cooled to 1323 K and water quenched after solution heating for 3.6 ksec at 1503 or 1523 K. Those of the second group were water quenched after solution heating for 3.6 ksec at 1503 or 1523 K. Those of the third group were furnace cooled to room temperature after solution heating for 3.6 ksec at 1503 K. The amount of GBR was 3 or 7% for the first group, 0% for the second group, and 13% for the third group, respectively. Before the creep test was started, these specimens were held for 10.8 ksec at a testing temperature of 1088 K. Therefore, it was considered that $M_{23}C_6$ carbides were present in the matrix in the specimens of the first and second groups, but to a lesser extent in the specimen of the third group. In general, the deformation resistance of the grains can be increased with the increase of carbides in matrix.

Fig. 12 shows the relations between the solution temperature and the creep rupture properties. The rupture life was longest in the specimens of the first group solution heated at 1523 K, which contained about 7% GBR nodules and $M_{23}C_6$ carbides in the matrix. The elongation and the reduction of area of the specimen were larger than that of the simply water quenched specimens solution heated at 1523 K, which

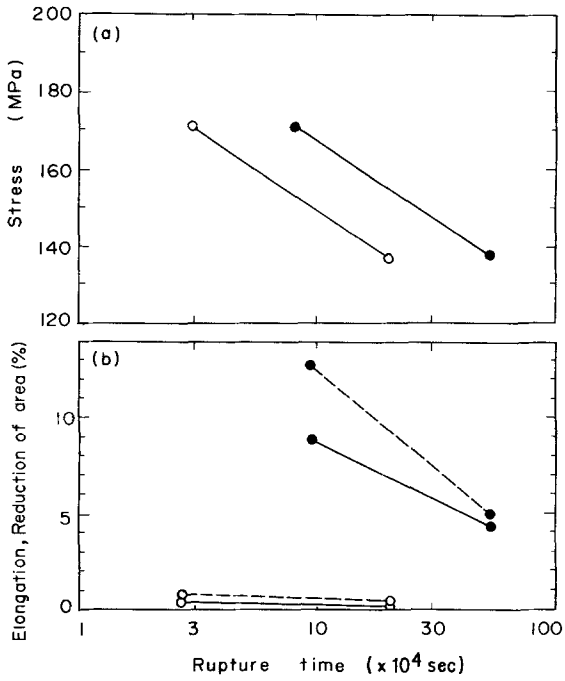


*Figure 13* Creep rupture properties of group 1, (●) 1523 K for 3.6 ksec, furnace cooled to 1323 K then water quenched; and group 2, (○) 1523 K for 3.6 ksec then water quenched; specimens of HS-21 alloy at 1088 K. (——) reduction in area, (– – –) elongation.

contained only the matrix precipitates. The elongation of the furnance cooled specimen, which involved about 13% GBR with a low amount of carbides in the matrix, was largest in the specimens tested, but the rupture life of it was shortest among them. Fig. 13 shows the creep rupture properties of the specimens of the first group and the second group. The rupture life of the specimens of the first group was about three times longer than that of the specimens of the second group, and the elongation of the former was also larger than that of the latter.

Fig. 14 shows the optical and scanning electron micrographs of ruptured specimens under a creep stress of 137 MPa at 1088 K. The direction of creep loading is horizontal in Fig. 14a, c and e. Large intergranular cracks and brittle intergranular fracture surface were observed on the specimens of the second group Fig. 14c and d, while small intergranular cracks were observed at the grain boundary in the specimen of the first group (Fig. 14a). Moreover, ledges, of which the width was about 20 $\mu$m, and dimples were also visible on the fracture surface of this specimen (Fig. 14b). Therefore, it is obvious that the grain boundary serration caused by GBR retarded the brittle intergranular fracture effectively, so that the rupture life of the specimen of the first group was longer than that of the specimen of the second group. In contrast, the rupture life of the specimen of the third group was shortest as shown in Fig. 12, though the GBR occurred about 13% with considerable grain boundary serration. The grain near the fracture surface was largely elongated along the loading axis, and a dimple pattern was observed on the fracture surface in this specimen (Fig. 14e and f). This can be attributed to the fact that the creep resistance of the third group with a smaller amount of carbides in the matrix is lower than that of

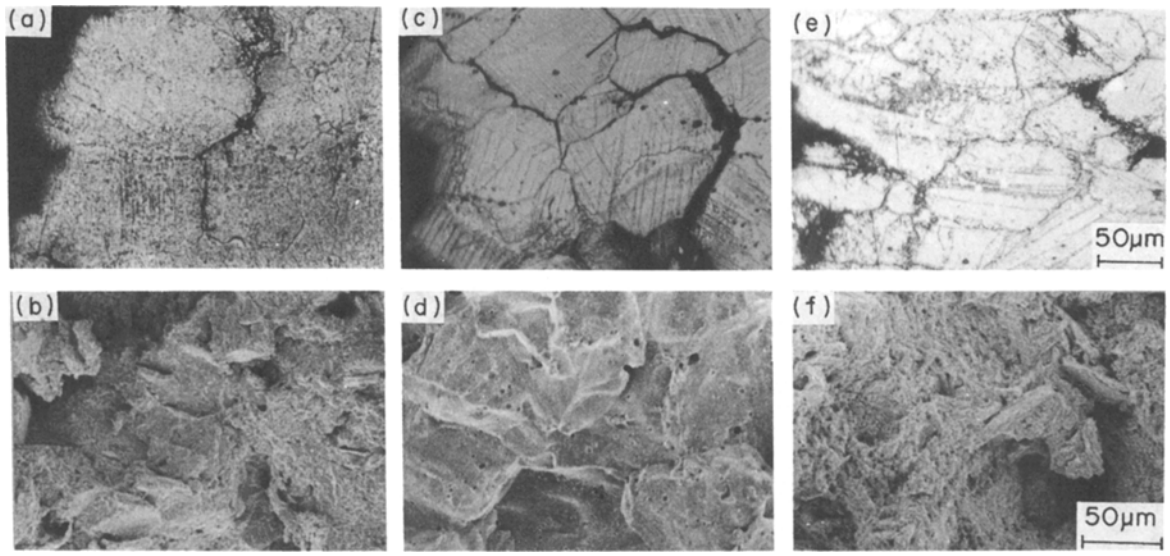


*Figure 14* Optical and scanning electron micrographs of HS-21 alloy creep ruptured at 1088 K, 137 MPa. (a) and (b) show the micrographs of group 1 specimens solution heated at 1523 K, (c) and (d) show those of group 2 specimens solution heated at 1523 K and (e) and (f) show those of group 3 specimens.

the first group or the second group with a large amount of the carbides. It is obvious, therefore, that the strengthening of the interior of grains due to the matrix precipitation is necessary to improve the creep rupture life together with the toughening of grain boundary due to the GBR [17].

## 4. Conclusions

The effects of solution temperature, cooling procedure and ageing treatment on grain boundary reaction (GBR) and matrix precipitation were examined in a wrought Co-base heat resisting superalloy HS-21. Then, the influences of the GBR and the matrix precipitation on creep rupture properties were investigated at 1088 K in air. The results obtained are summarized as follows:

1. GBR occurred considerably during furnace cooling from solution temperature, most of it occurred during cooling in the temperature range from 1373 to 1173 K. Grain boundaries were considerably serrated in a sample with an amount of GBR of above about 7% in area fraction. The extent of GBR that occurred during furnace cooling was also affected by the solution temperature, and it was large in the solution temperature range from 1523 to 1558 K. The matrix carbides scarcely formed in samples furnace cooled after solution heating.

2. GBR also occurred during ageing. Cooling procedure after solution heating had a extremely large effect on the GBR and the matrix precipitation during ageing. The GBR occurred considerably during ageing in the directly quenched sample. The maximum amount in the air cooled sample was about one-third of that in the directly quenched one. The precipitates in the matrix were easier to occur in the former than in the latter. Moreover, the GBR hardly occurred and the matrix precipitation occurred considerably in the water quenched sample. The GBR and the matrix precipitation were influenced by the dislocation density in the interior of grains which were different with cooling procedure. The amount of GBR tended to decrease under the conditions where the carbides in the matrix formed to a considerable extent.

3. The activation energy of the early stage of GBR was 244 kJ $mol^{-1}$. This is considered to be that of grain boundary diffusion of chromium.

4. Creep rupture life was longest for the specimen, which contains a small amount of GBR nodules (about 7% in area fraction) as well as a large extent of matrix precipitates in the interior of grains. This improvement of rupture life resulted from the retardation of brittle intergranular fracture due to the serrated grain boundaries with GBR and the strengthening of the interior of grains by the matrix precipitation.

## Acknowledgements

The authors wish to express their gratitude to Professor Ohmi Miyagawa of the Tokyo Metropolitan University for his helpful suggestions. Gratitude is also expressed to Mr Humio Ashihara, technical officer of Akita University, Takaaki Akasaka and Akihiko Miura, graduates of Akita University, who performed some of the experimental work, and to Mr Hiroyasu Goto of Mitsubishi Metal Corporation for supply of the experimental material.

## References

1. S. TAKEDA and N. YUKAWA, *Bull. Jpn. Inst. Met.* **6** (1967) 783.
2. H. HAMANAKA, *ibid.* **23** (1984) 238.
3. C. YAKER and C. A. HOFFMAN, National Advisory Committee for Aeronautics, Technical Note **2320** (1951).
4. C. A. HOFFMAN and C. F. ROBARDS, *ibid.* **2513** (1951).
5. N. J. GRANT and J. R. LANE, *Trans. ASM* **41** (1949) 95.
6. R. N. TAYLOR and R. B. WATERHOUSE, *J. Mater. Sci.* **18** (1983) 3265.
7. J. W. WEETON and R. A. SIGHORELLI, *Trans. ASM* **47** (1955) 815.
8. K. RAJAN, *Metall. Trans.* **13A** (1982) 1161.

9. J. B. VANDER SANDE, J. R. COKE and J. WULFF, *ibid.* **7A** (1976) 389.
10. M. KOBAYASHI, M. TANAKA, O. MIYAGAWA, T. SAGA and D. FUJISHIRO, *Tetsu-to-Hagane* **58** (1972) 1984.
11. R. WATANABE, in "Precipitation of Alloy" (Maruzen, Tokyo, 1972) p. 223.
12. M. TANAKA, O. MIYAGAWA, T. SAKAKI and D. FUJISHIRO, *J. Jpn. Inst. Met.* **40** (1976) 543.
13. M. YAMAZAKI, *ibid.* **30** (1966) 1032.
14. B. D. CULLITY, in "X-ray Diffraction" translated by G. Matsumura, (AGNE, Tokyo, 1968) p. 392.
15. R. HASHIGUCHI and T. CHIKAZUMI, in "Crystal Lattice Defects" (Asakura, Tokyo, 1970) p. 181.
16. M. TANAKA, O. MIYAGAWA, T. SAKAKI and D. FUJISHIRO, *Tetsu-to-Hagane* **65** (1979) 939.
17. O. MIYAGAWA, M. KOBAYASHI and M. YAMAMOTO, *Rep. 123rd Com., Jpn. Soc. Prom. Sci.* **13** (1972) 31.

*Received 1 July*
*and accepted 1 October 1985*